Cell Reports
Physical Science

Article

Ligand-controlled stereodivergent proton migration in skipped enynes

Graphical abstract

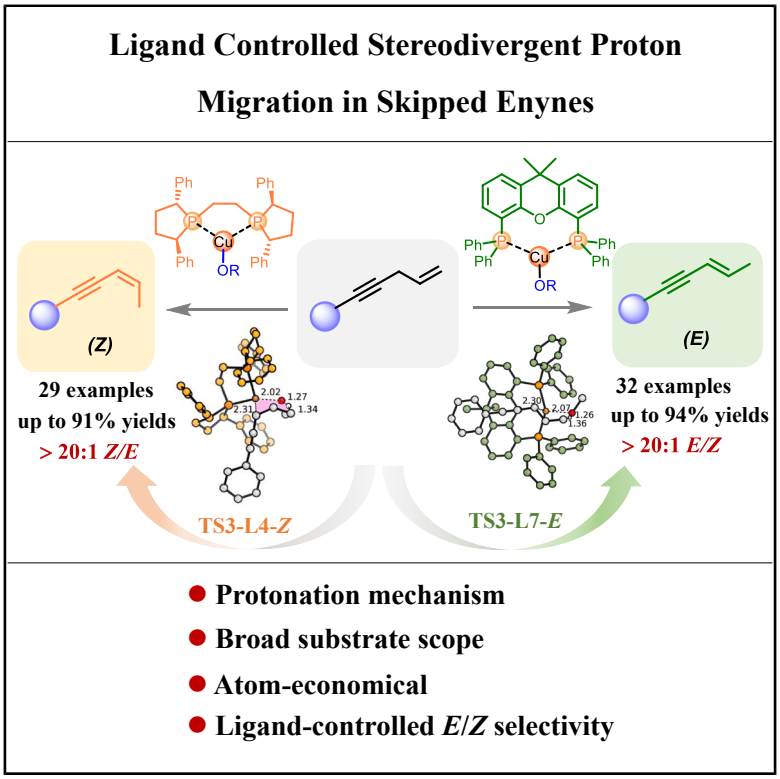

Highlights

- Copper(I)-catalyzed proton migration from skipped enynes to conjugated enynes is developed
- Synthesis of *E*- or *Z*-conjugated 1,3-enynes with good substrate scope and high *Z*/*E* selectivity
- DFT calculations rationalize the ligand effects in regio- and stereoselectivity

Authors

Tianle Wu, Chunying Fan, Weiwei Jin, ..., Kristin A. Persson, Pengchen Ma, Xiaofeng Wei

Correspondence

fanchunying1213@xjtu.edu.cn (C.F.), mapengchen2020@gmail.com (P.M.), xiaofeng.wei@xjtu.edu.cn (X.W.)

In brief

Conventional double-bond migration strategies predominantly depend on precious-metal hydrides or radical intermediates. Wu et al. report a copper-catalyzed, ligand-controlled proton migration process that enables stereodivergent synthesis of conjugated enynes from skipped enynes, introducing an innovative approach to transform abundant hydrocarbon feedstocks into high-value molecules via C–H reconstitution.

Wu et al., 2025, Cell Reports Physical Science *6*, 103020
December 17, 2025
https://doi.org/10.1016/j.xcrp.2025.103020

CellPress

Cell Reports
Physical Science

CellPress
OPEN ACCESS

Article

Ligand-controlled stereodivergent proton migration in skipped enynes

Tianle Wu,[1,10] Chunying Fan,[1,10,*] Weiwei Jin,[2,10] Xiaowei Xie,[3,9] Shaohong Wang,[4] Huishuang Wang,[1] Guangrui Shi,[1] Yuchen Gao,[5] Jiajia Sun,[1] Yunyi Zhao,[1] Yohei Shimizu,[6] Motomu Kanai,[7] Kristin A. Persson,[3,9] Pengchen Ma,[8,*] and Xiaofeng Wei[1,11,*]

[1]School of Pharmacy, Xi'an Jiaotong University, No.76, Yanta West Road, Xi'an, Shaanxi 710061, China
[2]General Surgery, Cancer Center, Department of Gastrointestinal and Pancreatic Surgery, Zhejiang Provincial People's Hospital (Affiliated People's Hospital), Hangzhou Medical College, Hangzhou, Zhejiang 310014, China
[3]Department of Chemistry, University of California, Berkeley, Berkeley, CA, USA
[4]Hubei Key Laboratory of Energy Storage and Power Battery, School of Mathematics, Physics and Optoelectronic Engineering, Hubei University of Automotive Technology, Shiyan, Hubei 442002, China
[5]Department of Urology, Shanghai Tenth People's Hospital, School of Medicine, Tongji University, Shanghai 200072, China
[6]Department of Chemistry, Faculty of Science, Hokkaido University, Sapporo, Hokkaido 060-0810, Japan
[7]Laboratory of Synthetic Organic Chemistry, Graduate of Pharmaceutical Sciences, The University of Tokyo, 7-3-1 Hongo, Bunkyo-ku, Tokyo 113-0033, Japan
[8]School of Chemistry, Xi'an Jiaotong University, Xi'an, Shaanxi 710049, China
[9]Materials Science Division, Lawrence Berkeley National Laboratory, Berkeley, CA 94720, USA
[10]These authors contributed equally
[11]Lead contact
*Correspondence: fanchunying1213@xjtu.edu.cn (C.F.), mapengchen2020@gmail.com (P.M.), xiaofeng.wei@xjtu.edu.cn (X.W.)
https://doi.org/10.1016/j.xcrp.2025.103020

SUMMARY

Having full control over the regio- and stereoselective isomerization of C=C double bonds is essential for accessing stereochemically defined olefins. However, most of the double-bond migration techniques used in the past decades have relied on precious-metal hydrides or radical-based approaches. These methods often suffer from reversible equilibria, hydrogen scrambling, incomplete *E*/*Z* selectivity, and high costs. Herein, we demonstrate a nonprecious, reductant-free, and atom-economical copper(I)-catalyzed regioselective and stereodivergent proton migration in skipped enynes. The developed method demonstrates high functional group compatibility and good *Z*/*E* selectivity under mild conditions and provides a variety of *E*- or *Z*-conjugated 1,3-enynes. Mechanistic and density functional theory (DFT) studies reveal the ligand-controlled proton migration process in detail.

INTRODUCTION

Olefins are widely used functional groups in the materials, pharmaceuticals, and food industries, serving as crucial chemical building blocks for various transformations.[1,2] The geometric arrangement of olefin π-bonds significantly influences their function, with examples like *trans* rosuvastatin (Crestor) showing enhanced anti-cardiovascular disease performance[3,4] and *cis*-configured (+)-discodermolide dominating microtubule-stabilizing ability,[5] while switching the olefin configuration significantly decreased the bioactivity (Scheme 1A). Therefore, achieving the selective and well-defined construction of alkenes is of utmost importance. Among the numerous synthetic methods for incorporating olefins,[6–12] one promising approach is the isomerization of existing C=C double bonds through regio- and stereoselective proton transfer. Four general mechanisms for metal-catalyzed alkene isomerization are proposed, namely, the alkyl-,[13–17] π-allyl-,[18–22] hydrogen atom transfer (HAT)-,[23] and metalloradical-induced H atom relocation mechanisms[24–28] (Scheme 1B, a–d). Despite these achievements, the *E*/*Z* selectivity often remains incomplete, leading to challenging purification processes. Additionally, few studies have succeeded in simultaneously controlling the *E*/*Z* selectivity of olefins[29–32] (Scheme 1C). Recently, the Engle and Vantourout groups developed an Ni-H-mediated insertion/elimination approach that selectively controls *Z*- or *E*-isomerization of terminal alkenes. Although this approach is effective for various terminal alkenes, it is less successful with styrenyl alkynes, which yield only *Z*-1,3-enynes with moderate efficiency and a *Z*/*E* ratio of 82:18. This method does not provide access to *E*-1,3-enynes, which are valuable intermediates for synthesizing functional materials and bioactive compounds such as terbinafine,[33–35] diabetes treatment candidate NNC 61-4655,[36,37] and bioactive constituents isolated from *Asparagus cochinchinensis*[36] (Scheme 1A). Few examples demonstrate effective, stereodivergent *Z*/*E* selectivity for the synthesis of conjugated 1,3-enynes.[37–39] In 2018, Zhao and co-workers reported the catalytic effects of iron(II) complexes with functionalized amine-pyrazolyl tripodal

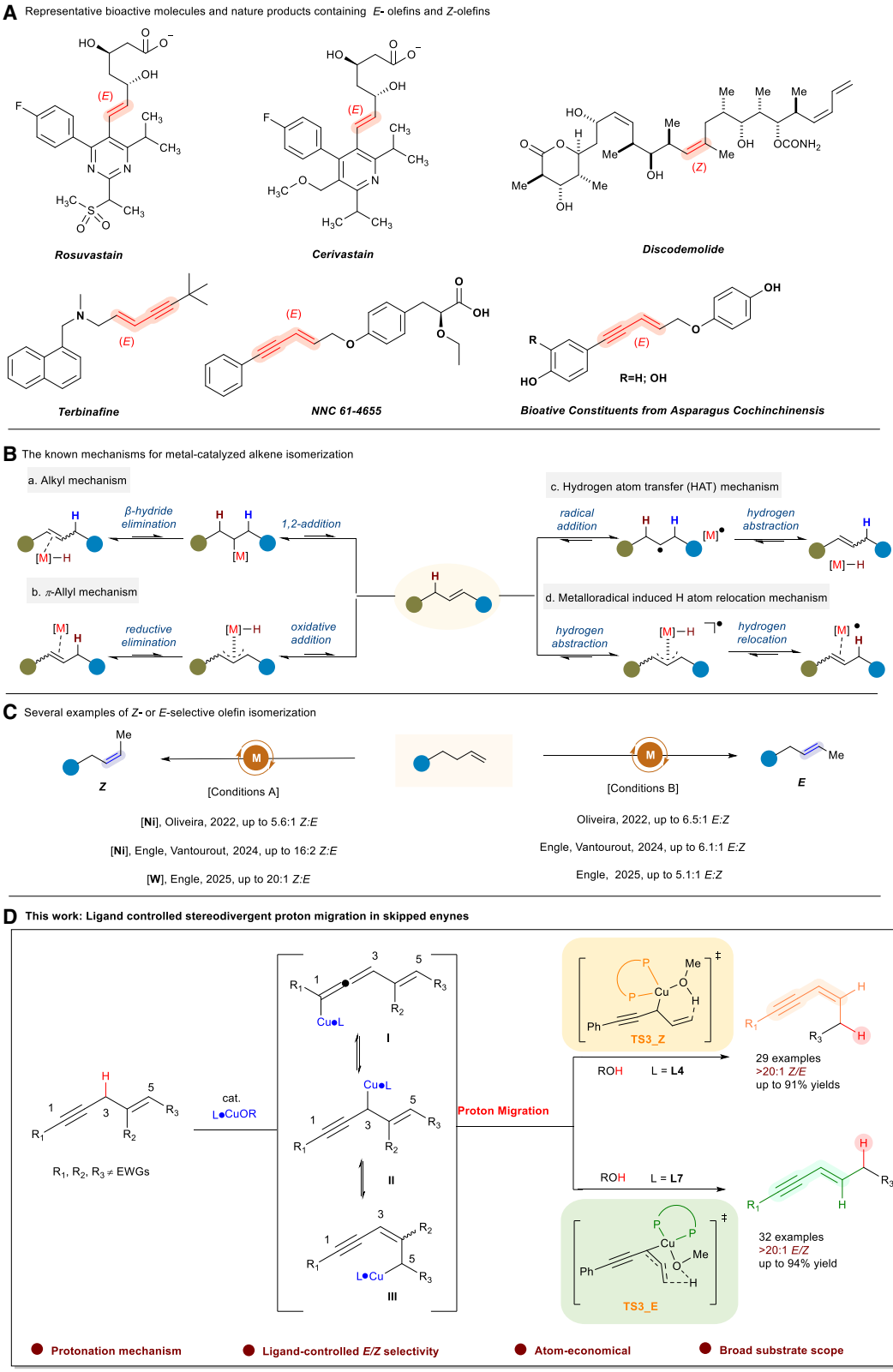

(legend on next page)

Table 1. Optimization of the reaction conditions

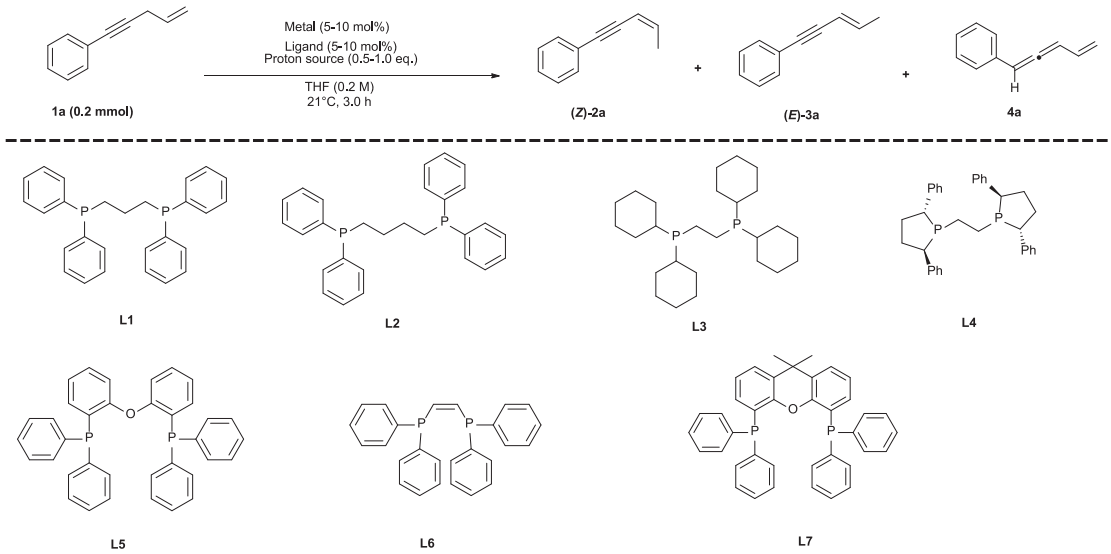

Entry[a]	Metal (%)	Ligand (%)	Proton source (equiv)	Yield of (*Z*)-**2a** + (*E*)-**3a** (%)[b]	Yield of (**4a**) (%)[b]	(*Z*)-**2a**:(*E*)-**3a**[c]
1	MesCu (5)	**L1** (5)	^{t}BuOH (1.0)	trace	–	–
2	MesCu (5)	**L2** (5)	^{t}BuOH (1.0)	trace	–	–
3	MesCu (5)	**L3** (5)	^{t}BuOH (1.0)	trace	–	–
4	MesCu (5)	**L4** (5)	^{t}BuOH (1.0)	89	0	>20:1
5	MesCu (5)	**L5** (5)	^{t}BuOH (1.0)	trace	–	–
6	MesCu (5)	**L6** (5)	^{t}BuOH (1.0)	20	53	1:1
7	MesCu (5)	**L7** (5)	^{t}BuOH (1.0)	20	66	1:2
8	MesCu (5)	**L7** (5)	MeOH (1.0)	73	19	1:11
9	MesCu (5)	**L4** (5)	MeOH (0.5)	82	12	>20:1
10[d]	MesCu (10)	**L7** (10)	MeOH (0.5)	93	–	1:12
11[d]	MesCu (10)	**L7** (10)	^{i}PrOH (0.5)	91	–	1:5
12[d]	MesCu (10)	**L7** (10)	EtOH (0.5)	83	10	1:8
13[d]	–	**L7** (10)	MeOH (0.5)	0	–	–
14[d]	MesCu (10)	–	MeOH (0.5)	0	–	–
15[d]	MesCu (5)	**L7** (5)	–	0	–	–
16	MesCu (5)	–	^{t}BuOH (1.0)	0	–	–
17	MesCu (5)	**L4** (5)	–	0	–	–
18	–	**L4** (5)	^{t}BuOH (1.0)	0	–	–

[a]General reaction conditions: metal (5–10 mol %), ligand (5–10 mol %), and proton source (0.5–1.0 equiv) were reacted in tetrahydrofuran (THF) (1.0 mL) at room temperature for 10 min. Then, **1a** (0.2 mmol) was added and reacted for 3.0 h under argon.
[b]Yields were determined by ^{1}H-NMR analysis of the crude mixture using N,N-dimethylformamide as an internal standard.
[c]The *Z*/*E* ratios were determined by ^{1}H-NMR analysis of the crude mixture.
[d]Reaction time was 1.0 h at 0°C–5°C.

ligands, achieving KO^{t}Bu- and NaO^{t}Bu-mediated *E*/*Z* selectivity during terminal aryl alkyne dimerization.[39] However, the scope was limited to aromatic substrates with limited *Z*/*E* selectivity. To date, general catalytic methods promoting stereodivergent proton migration from skipped enynes to conjugated 1,3-enynes, providing both *E*- and *Z*-isomers with high selectivity,

Scheme 1. Relevance, precedents, and synopsis of work
(A) Representative bioactive molecules and natural products containing *E*-olefins and *Z*-olefins.
(B) The known mechanisms for metal-catalyzed alkene transposition.
(C) Several examples of *Z*- or *E*-selective olefin isomerization.
(D) This work: ligand-controlled stereodivergent proton migration in skipped enynes.

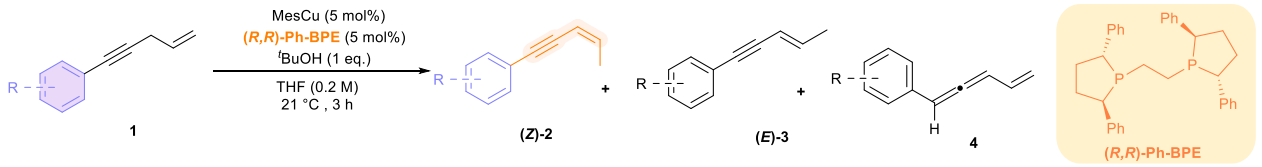

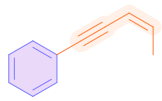
(Z)-2a
83% yield, Z/E>20:1
(2+3):4=11:1

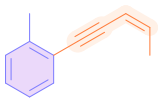
(Z)-2b
89% yield, Z/E>20:1
(2+3):4>20:1

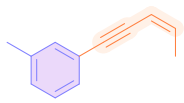
(Z)-2c
78% yield, Z/E>20:1
(2+3):4>20:1

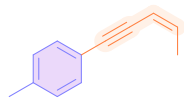
(Z)-2d
86% yield, Z/E>20:1
(2+3):4=9:1

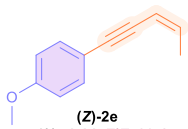
(Z)-2e
74% yield, Z/E>20:1
(2+3):4=13:1

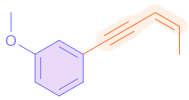
(Z)-2f
84% yield, Z/E>20:1
(2+3):4=14:1

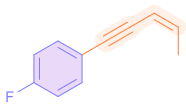
(Z)-2g
70% yield, Z/E>20:1
(2+3):4=5:1

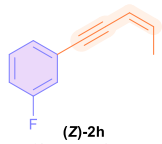
(Z)-2h
79% yield, Z/E>20:1
(2+3):4>20:1

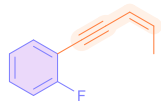
(Z)-2i
86% yield, Z/E>20:1
(2+3):4>20:1

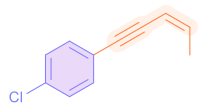
(Z)-2j
78% yield, Z/E>20:1
(2+3):4=5:1

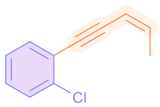
(Z)-2k
76% yield, Z/E>20:1
(2+3):4>20:1

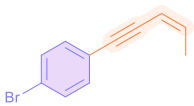
(Z)-2l
71% yield, Z/E>20:1
(2+3):4=3:1

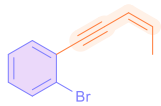
(Z)-2m
79% yield, Z/E>20:1
(2+3):4=11:1

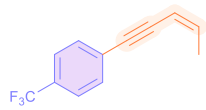
(Z)-2n
76% yield, Z/E>20:1
(2+3):4=4:1

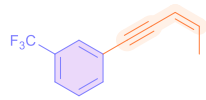
(Z)-2o
64% yield, Z/E>20:1
(2+3):4=5:1

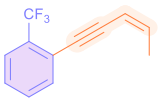
(Z)-2p
78% yield, Z/E>20:1
(2+3):4=18:1

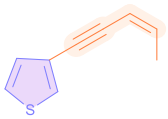
(Z)-2q
80% yield, Z/E>20:1
(2+3):4>20:1

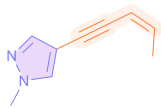
(Z)-2r
83% yield, Z/E>20:1
(2+3):4=10:1

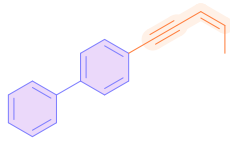
(Z)-2s
86% yield, Z/E>20:1
(2+3):4>20:1

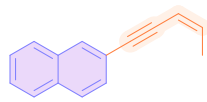
(Z)-2t[a]
85% yield, Z/E>20:1
(2+3):4>20:1

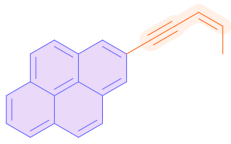
(Z)-2u
79% yield, Z/E>20:1
(2+3):4>20:1

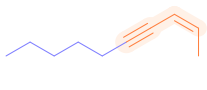
(Z)-2v
86% yield, Z/E>20:1
(2+3):4=11:1

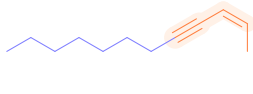
(Z)-2w
78% yield, Z/E>20:1
(2+3):4=4:1

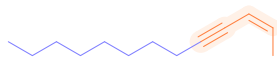
(Z)-2x
81% yield, Z/E>20:1
(2+3):4>20:1

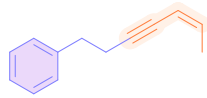
(Z)-2y[a]
31% yield, Z/E>20:1
(2+3):4>20:1

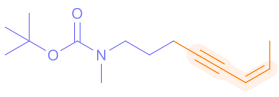
(Z)-2z
60% yield, Z/E>20:1
(2+3):4=7:1

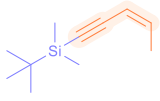
(Z)-2aa
91% yield, Z/E>20:1
(2+3):4>20:1

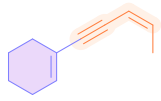
(Z)-2ab
83% yield, Z/E>20:1
(2+3):4=18:1


(Z)-2ac[a]
58% yield, Z/E >20:1
(2+3):4>20:1

Scheme 2. Substrate scope of (*Z*)-1,3-enyne under proton transfer conditions

General reaction conditions: MesCu (0.01 mmol), (*R,R*)-Ph-BPE (0.01 mmol), and ^{t}BuOH (0.2 mmol) were reacted in THF (1.0 mL) at room temperature for 10 min. Then, **1** (0.2 mmol) was added and reacted for 3.0 h at 21°C. Isolated yields. The *Z*/*E* ratios and [(**2**+**3**):**4**] were determined by ^{1}H-NMR analysis of the crude reaction mixture.

[a]Reaction was conducted using 10 mol % (0.02 mmol) of MesCu/(*R,R*)-Ph-BPE loading.

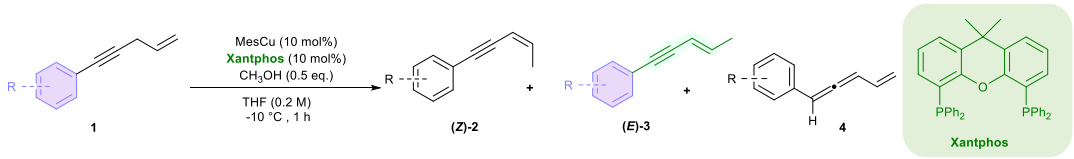

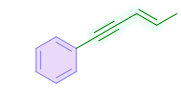
(*E*)-3a[a]
93% yield, *E*/*Z* = 11:1
(2+3):4>20:1

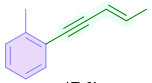
(*E*)-3b
91% yield, *E*/*Z* = 10:1
(2+3):4>20:1

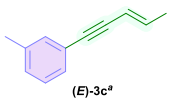
(*E*)-3c[a]
92% yield, *E*/*Z* = 10:1
(2+3):4>20:1

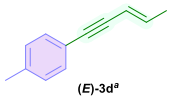
(*E*)-3d[a]
90% yield, *E*/*Z* = 9:1
(2+3):4>20:1

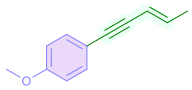
(*E*)-3e
81% yield, *E*/*Z* = 18:1
(2+3):4>20:1

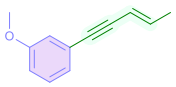
(*E*)-3f
83% yield, *E*/*Z* = 12:1
(2+3):4>20:1

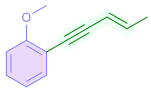
(*E*)-3g
80% yield, *E*/*Z* = 11:1
(2+3):4>20:1

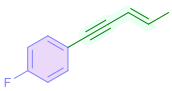
(*E*)-3h
94% yield, *E*/*Z* = 8:1
(2+3):4>20:1

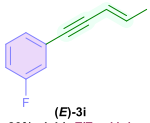
(*E*)-3i
89% yield, *E*/*Z* = 11:1
(2+3):4>20:1

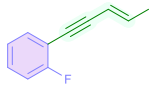
(*E*)-3j
88% yield, *E*/*Z* = 8:1
(2+3):4>20:1

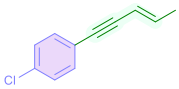
(*E*)-3k
86% yield, *E*/*Z* = 11:1
(2+3):4>20:1

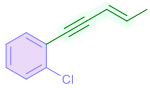
(*E*)-3l[a]
83% yield, *E*/*Z* = 6:1
(2+3):4>20:1

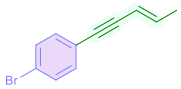
(*E*)-3m
88% yield, *E*/*Z* = 7:1
(2+3):4=14:1

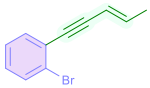
(*E*)-3n
85% yield, *E*/*Z* = 7:1
(2+3):4>20:1

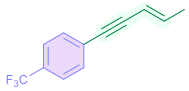
(*E*)-3o
88% yield, *E*/*Z* >20:1
(2+3):4>20:1

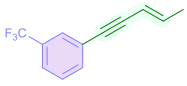
(*E*)-3p
86% yield, *E*/*Z* = 6:1
(2+3):4>20:1

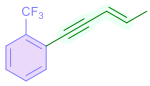
(*E*)-3q
84% yield, *E*/*Z* = 6:1
(2+3):4>20:1

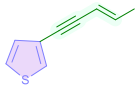
(*E*)-3r
92% yield, *E*/*Z* = 11:1
(2+3):4>20:1

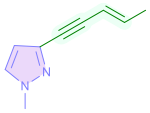
(*E*)-3s[a]
90% yield, *E*/*Z* = 6:1
(2+3):4>20:1

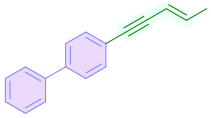
(*E*)-3t
89% yield, *E*/*Z* = 9:1
(2+3):4>20:1

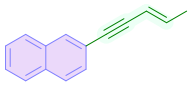
(*E*)-3u[b]
91% yield, *E*/*Z* = 8:1
(2+3):4=14:1

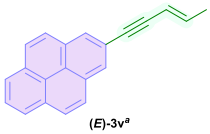
(*E*)-3v[a]
90% yield, *E*/*Z* = 6:1
(2+3):4>20:1


(*E*)-3w
36% yield, *E*/*Z* >20:1
(2+3):4>20:1

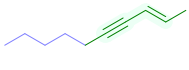
(*E*)-3x
91% yield, *E*/*Z* = 5:1
(2+3):4>20:1

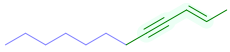
(*E*)-3y
88% yield, *E*/*Z* = 5:1
(2+3):4>20:1

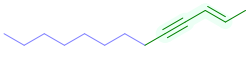
(*E*)-3z
86% yield, *E*/*Z* = 8:1
(2+3):4>20:1

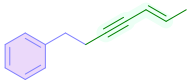
(*E*)-3aa[a,b]
32% yield, *E*/*Z* = 6:1
(2+3):4>20:1


(*E*)-3ab
38% yield, *E*/*Z* >20:1
(2+3):4>20:1

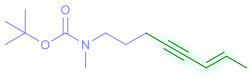
(*E*)-3ac[a,b]
64% yield, *E*/*Z* = 6:1
(2+3):4>20:1

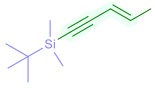
(*E*)-3ad[a,b,c]
79% yield, *E*/*Z* = 11:1
(2+3):4>20:1

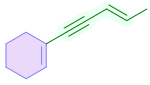
(*E*)-3ae[a]
94% yield, *E*/*Z* = 7:1
(2+3):4>20:1

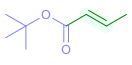
(*E*)-3af
61% yield, *E*/*Z* >20:1
(2+3):4>20:1

(legend on next page)

remain an unsolved challenge. The lack of progress may be attributed to limited reaction patterns and ligands that effectively support the metal center during the reaction to precisely deliver the proton atom.

We are intrigued by the transition-metal-catalyzed redox-neutral proton migration approach, due to its apparent simplicity, while also recognizing the fundamental complexity involved in achieving regioselectivity during the protonation step. Among various catalyst options, copper stands out for its advantages of being abundantly available, cost-effective, and environmentally sustainable. The σ or π coordination ability of copper complexes with a wide range of functional groups, along with the versatility in selecting mono- and bidentate ligands, makes them powerful tools for ligand-controlled proton migration.[40] While copper-catalyzed direct vinylogous reactions offer an alternative method for installing olefins,[41] the stereoselectivity is generally determined by the intermolecular C–C-bond-forming process, with a well-established six-member-ring transition state,[42–45] and stereo-switchable olefin isomerization via catalyst-controlled direct protonation has not been established so far. In our previous work, we identified a novel chiral ferrocenyl phosphine ligand that enabled regio- and enantioselective proton migration of skipped enynes, presenting a new concept for converting readily available and abundant hydrocarbon feedstocks into high-value-added molecules through C–H reconstitution.[46] In this context, we envision that employing a copper catalyst with precisely designed coordination patterns will allow us to switch the regioselectivity from C1 to C5, leading to the synthesis of bioactive *cis*- or *trans*-conjugated enynes in a catalyst-controlled, stereodivergent manner (Scheme 1D).

RESULTS AND DISCUSSION

Optimization of reaction conditions

Based on the above-mentioned working hypothesis, we initiated our investigation using 1-phenyl-4-penten-1-yne (**1a**) as a model substrate, alcohols as a proton source, and a 5–10 mol % catalyst loading (Table 1). After preliminary experiments on copper sources, phosphorus ligands, and proton sources (entries 1–7; supplemental methods; Tables S1 and S2), we found that employing 5 mol % of mesitylcopper (MesCu) and (*R,R*)-Ph-BPE (**L4**), with ^{t}BuOH as the proton source, afforded *Z*-selective conjugated enyne (*Z*)-**2a** in 89% yield and with >20:1 *Z*/*E* selectivity (entry 4). During ligand evaluation, the replacement of **L4** with Xantphos (**L7**) was found to switch product selectivity from (*Z*)-**2a** to (*E*)-**3a** in a 1:2 *Z*/*E* ratio (entry 7). To improve *E*-selectivity, we examined common alcohol proton sources, such as MeOH, EtOH, ^{i}PrOH, etc. Surprisingly, using MeOH as the proton source led to the highest *E*-selectivity (*E*/*Z* = 1:12) and an excellent yield (93%) (entries 10–12). Control experiments indicated that MesCu, ligand **L4** or **L7**, and proton source ^{t}BuOH or MeOH were all essential reagents (entries 13–18). Additionally, we explored the dependency on reaction parameters, catalyst dosage, reaction temperature, concentration, and other conditions (supplemental methods; Tables S3–S9). Consequently, both stereoisomers, (*Z*)-**2a** and (*E*)-**3a**, were selectively accessible in high yields and stereodivergency simply by switching the type of bidentate phosphine ligand for the copper catalyst.

Substrate scope

Next, we explored the substrate scope of the reaction under the optimized conditions, using 5–20 mol % catalyst, depending on the substrate reactivity (Schemes 2 and 3). Our investigations revealed that the general reaction conditions tolerated a diverse array of functional groups. Various skipped enynes with electron-donating substituents (methyl and methoxy) at *ortho*-, *meta*-, or *para*-positions (**2b–2f** and **3b–3g**) were tolerated. Halogen substituents, such as fluoride (**2g–2i** and **3h–3j**), chloride (**2j**, **2k**, **3k**, and **3l**), and bromide (**2l**, **2m**, **3m**, and **3n**), as well as electron-deficient trifluoromethyl (**2n–2p** and **3o–3q**) groups, were efficiently converted to their corresponding isomers within 1.0–3.0 h, exhibiting excellent yields (70%–94%) and stereoselectivities (up to >20:1). Furthermore, heterocyclic compounds, such as thiophene and pyrazole (**2q**, **2r**, **3r**, and **3s**), were also effectively converted into the desired products. The scope was further expanded to other aromatic cores, such as biphenyl (**2s** and **3t**), naphthalene (**2t** and **3u**), and pyrene (**2u** and **3v**), all efficiently forming the desired products in 79%–91% yields and good stereoselectivity. Moreover, the substrate scope extended beyond aromatic compounds, as aliphatic compounds (**2v–2y** and **3x–3aa**; Schemes 2 and 3) and siliceous compounds (**2aa** and **3ad**; Schemes 2 and 3) were also amenable to the reaction. Even challenging substrates, such as aliphatic amines (**2z** and **3ac**; Schemes 2 and 3), could be converted to the corresponding products with good yields and stereoselectivity. In addition, compounds with halogen-substituted ends (**3w** and **3ab**; Scheme 3) can also be well transformed and widely used in subsequent derivatization. Overall, the stereodivergent proton migration strategy proceeded with excellent regioselectivity ((**2**+**3**):**4** > 20:1 was determined by ^{1}H-NMR analysis), providing the desired conjugated enyne products. It is also noteworthy that other olefins, such as tert-butyl but-3-enoate, could be isomerized to form the corresponding *trans* product (**2ac** and **3af**) in moderate yields and with >20:1 stereoselectivity.

Synthetic applications

The migration also exhibits excellent selectivity and efficiency on a 1-g scale (Scheme 4A): after obtaining the skipped enyne

Scheme 3. Substrate scope of (*E*)-1,3-enyne under proton transfer conditions

General reaction conditions: MesCu (0.02 mmol), Xantphos (0.02 mmol), and CH_3OH (0.1 mmol) were reacted in THF (1.0 mL) at room temperature for 10 min. Then, **1** (0.2 mmol) was added and reacted for 1.0 h at −10°C. Isolated yields. The *Z*/*E* ratios and [(**2**+**3**):**4**] were determined by ^{1}H-NMR analysis of the crude mixture.

[a]The reaction was conducted at 0°C–5°C.

[b]Reaction was conducted using 20 mol % of MesCu/Xantphos loading.

[c]0.5 equiv of magnesium di(2-propanolate) was used as additive.

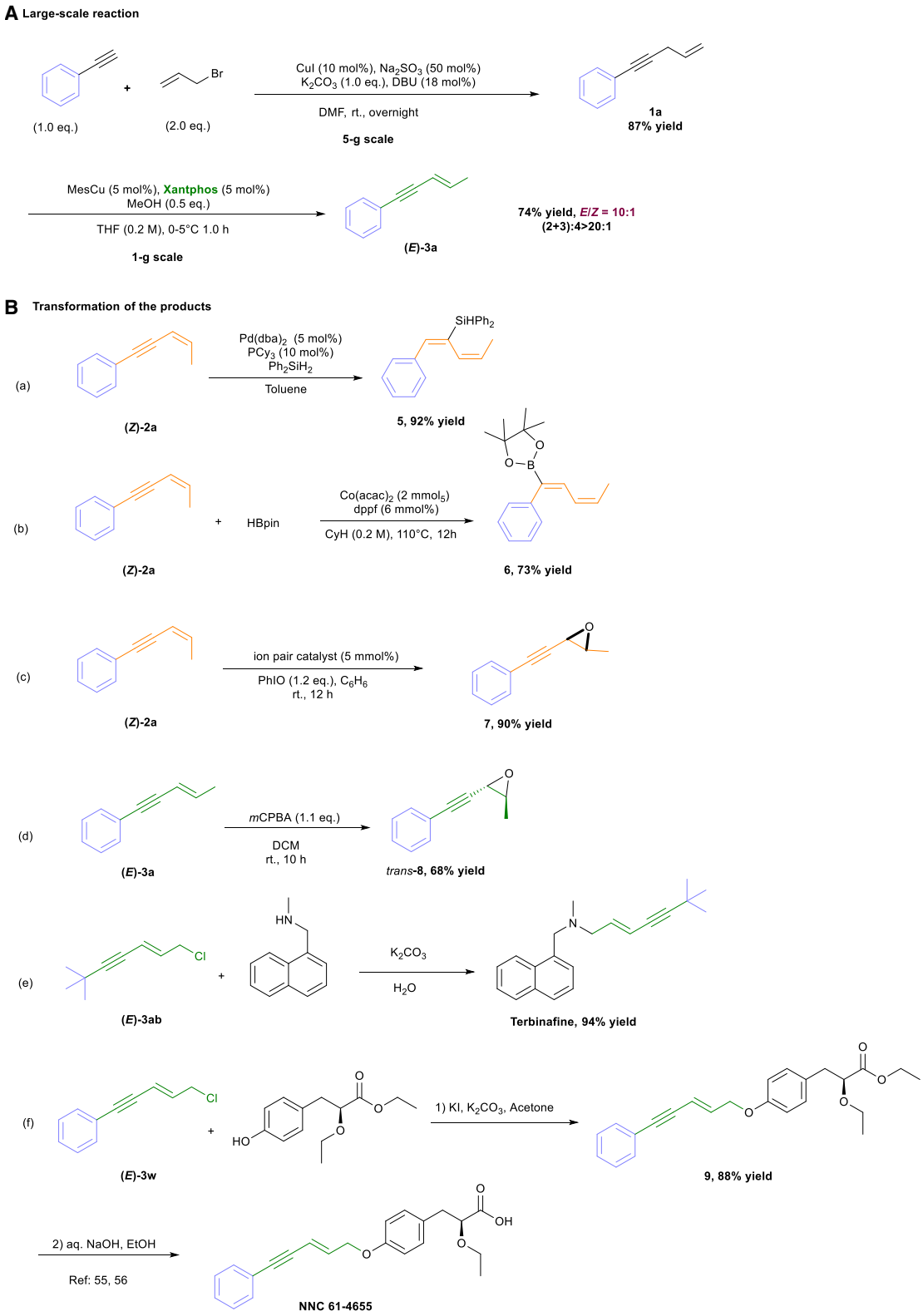

Scheme 4. Gram-scale reaction and synthetic utilities of final products

(A) Large-scale reaction.

(B) Transformation of the products.

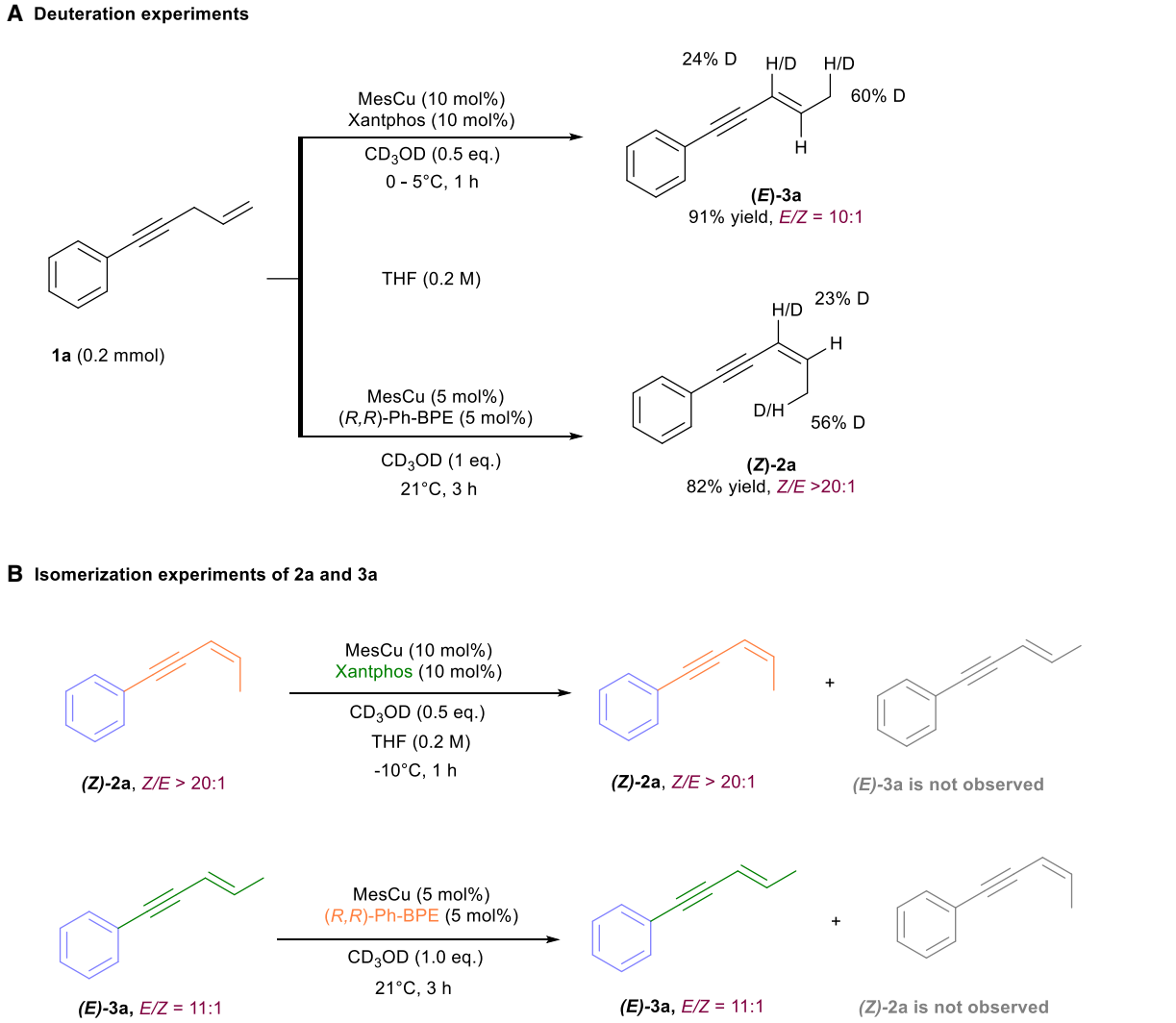

Scheme 5. Mechanism studies

(A) Deuteration experiments.

(B) Isomerization experiments of **2a** and **3a**.

1a through a copper-catalyzed substitution reaction,[47] the proton migration for the synthesis of conjugated enynes (*E*)-**3a** was carried out on a gram scale using 5 mol % catalyst at 0°C–5°C for 1.0 h. The reaction proceeded smoothly, yielding pure product (*E*)-**3a** in a 74% yield with perfect regioselectivity (*E*/*Z* = 10:1). The resulting product can be easily purified, making it an ideal method for the practical and straightforward synthesis of valuable 1,3-enynes from readily available starting materials.

To further demonstrate the synthetic utility of our protocol, we conducted several transformations of the conjugated enyne moiety (Scheme 4B). The *cis*-conjugated enyne moiety (*Z*)-**2a** can be selectively and stereoselectively converted into the *cis*-diene moiety through palladium-catalyzed hydrosilylation conditions, affording compound **5** in a high yield (Scheme 4B, a).[48] In addition, (*Z*)-**2a** can also be converted with HBpin into 1,3-dienylborate ester **6** in a 73% yield, which have important synthetic value (Scheme 4B, b).[49] The epoxidation of conjugated enyne (*Z*)-**2a** and (*E*)-**3a** led to the formation of the corresponding products in high yields (**7**: 90% and **8**: 68%) (Scheme 4B, c and d).[50–52] Moreover, this method was applied to the concise preparation of an antifungal drug, terbinafine, which contains the (*E*)-1,3-enyne structural moiety. Terbinafine exhibits strong antimycotic activity and is currently used for the treatment of skin mycoses.[35] Several strategies have been described, including the Pd-catalyzed Stille coupling of an (*E*)-vinyl iodide with an alkynyl tin and the Sonogashira coupling of an (*E*)-vinyl chloride with tert-butyl acetylene.[53,54] In our approach, we treated the (*E*)-1-chloro-6,6-dimethyl-2-heptene-4-yne ((*E*)-**3ab**, *E*/*Z* > 20:1) with *N*-methyl-1-naphthalenmethyamine in the presence of sodium carbonate. As expected, the desired terbinafine was obtained in a 94% isolated yield, showcasing the practicality and

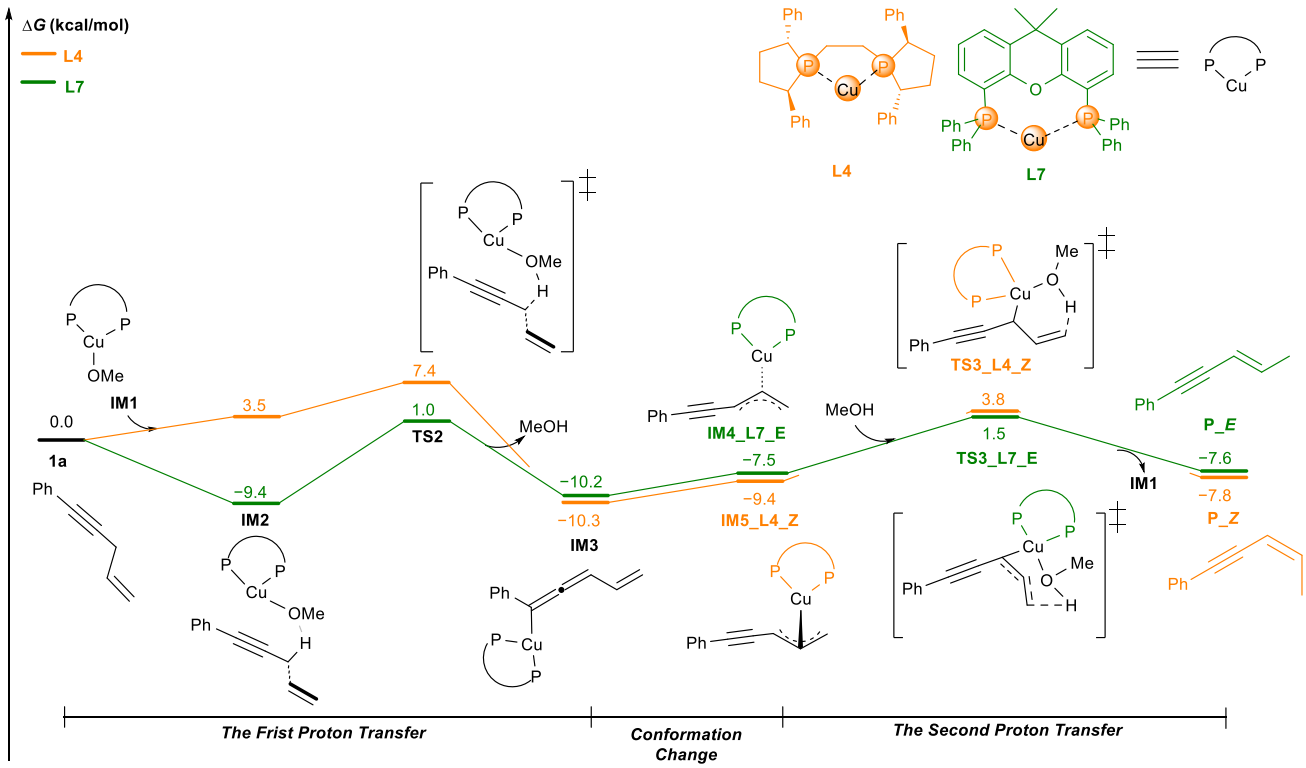

Figure 1. Gibbs free energy profile for the protonation of the carbon–carbon double bond catalyzed by the Cu catalyst with ligands

(*R,R*)-Ph-BPE (**L4**) and Xantphos (**L7**) ligands are in orange and green, respectively. 3D structures of key transition states are given, and the nonpolar hydrogens are hidden for clarity. Distances are given in angstroms (Å). See also Figure S4.

efficiency of our method (Scheme 4B, e). Additionally, we targeted a key intermediate, (*E*)-**3w**, in the synthesis of peroxisome proliferator-activated receptor (PPAR) agonist NNC 61-4655, which exhibits excellent pharmacokinetic properties and is considered a promising antidiabetic drug candidate.[34,55,56] By incorporating our copper-catalyzed proton migration protocol in the early steps of the synthesis, we achieved a shorter route to NNC 61-4655 through alkylation and hydrolysis of the ester (Scheme 4B, f). Apart from these representative examples, a conjugated enyne moiety offers a plethora of possibilities for further transformations, making it widely applicable in chemistry, biology, medicine, materials, and other fields.[57–61] Its prevalence as a structural element in various natural products and biologically active compounds makes it a pivotal building block for synthesizing diverse compounds, ranging from fine chemicals to functional polymers. Various functional groups, including conjugated olefins,[62] chiral propargylamines,[63] alkenylsilanes,[64] isoxazole derivatives,[65] and others,[66] can be efficiently synthesized through strategies such as regioselective reduction and stereodispersive tandem reactions starting from conjugated enynes. This opens up new avenues for developing innovative structures in organic materials and bioactive molecules.

Theoretical basis

To gain insight into the reaction mechanism, we conducted deuteration experiments using CD_3OD as a deuterium source (Scheme 5). When a Cu/Xantphos catalyst was employed, the *trans*-conjugated enyne product (*E*)-**3a** was obtained with deuteration at the C3 and C5 positions, while the *cis*-conjugated enyne product (*Z*)-**2a** showed a similar deuteration pattern, highlighting the crucial role of CD_3OD as the medium for proton migration. Notably, the allene product **4a**, achieved through deuteration at the C1 position, which was predominant in our previous work, was not observed in either case. These results provide valuable mechanistic insight, suggesting that the reprotonation of the intermediate organocopper species at the C3 position competes in both stereoselective proton migration pathways: from **1a** to (*E*)-**3a** with MesCu/Xantphos and from **1a** to (*Z*)-**2a** with MesCu/(*R,R*)-Ph-BPE. Furthermore, we conducted isomerization experiments of (*Z*)-**2a** and (*E*)-**3a**. The fact that (*Z*)-**2a** did not undergo stereoselective transformation under *E*-type reaction conditions and deuterium was not incorporated at the C1, C3, and C5 positions, while (*E*)-**3a** showed similar results under *Z*-type reaction conditions, rules out the possibility that (*Z*)-**2a** or (*E*)-**3a** was generated through *Z*/*E*-selective isomerization.

Density functional theory (DFT) calculations were performed to gain insights into the ligand control of *E*/*Z* selectivity in this reaction. As shown in Figure 1, the proton abstraction process of **1a** occurs with energy barriers of 7.4 kcal/mol with **L4** and 10.4 kcal/mol with **L7**. Notably, **intermediate** (**IM)2** with the **L7** ligand is more stable than with **L4** by 11.9 kcal/mol. **IM3** is formed with the release of one molecule of MeOH, followed by a conformational change (Figure S4), resulting in the relatively stable species **IM5_L4_*Z*** and **IM4_L7_*E*** (see 3D structures in Figure S2).

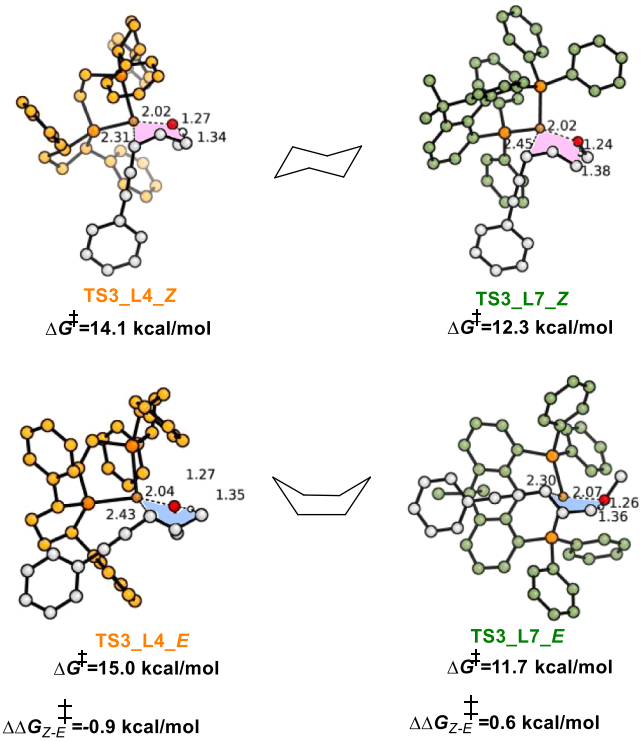

Figure 2. 3D structures of *Z*/*E* transition states and Gibbs free energies

L4 is in orange, and **L7** is in green. The nonpolar hydrogens are hidden for clarity. Distances are given in angstroms (Å). See also Figures S2 and S3.

IM5_L4_*Z* and **IM4_L7_*E*** lead to the final products **P_*Z*** and **P_*E*** through six-membered-ring transition states, with energy barriers of 14.1 and 11.2 kcal/mol, respectively, which agrees with the experimental observations. The catalyst (**IM1**) is released at the end of the reaction.

To further understand the role of the ligands **L4** and **L7** in controlling the *E*/*Z* selectivity, we investigated the transition-state energy barriers for the formation of *Z*/*E* products, as shown in Figure 2. With the **L4** ligand, the transition state leading to the *Z* conformer product is favored by 0.9 kcal/mol energy compared to the *E* conformer product. Conversely, with the **L7** ligand, the situation is reversed: the energy barrier for the formation of the conformer *E* product is 1.9 kcal/mol lower than that for the *Z* conformer product. This difference is likely due to steric effects between the ligand and the substrate[46,67–70] (see the noncovalent interaction analysis in supplemental methods and Figure S3).

In conclusion, we have presented a novel strategy for the stereodivergent synthesis of conjugated enynes through copper-catalyzed proton migration from skipped enynes. Our findings suggest a mechanistic pathway involving the activation of sp^3–C–H bonds in readily available hydrocarbon skipped enynes under mild conditions, independent of electron-withdrawing groups (EWGs). Theoretical DFT calculations support a catalyst-controlled proton-transfer process, facilitated by ^{t}BuOH/MeOH, and indicate the importance of ligands (**L4**/**L7**) in controlling both the regio- and stereoselectivity of this reaction. This method introduces an innovative concept for transforming readily available and abundant hydrocarbon feedstocks into high-value-added molecules through C–H reconstitution.

Limitations of the study

Despite its broad applicability, our protocol could not be successfully applied to skipped enynes with terminal methyl (**1aq**), dimethyl (**1ar**), or phenyl (**1as**) substituents, as well as heterocyclic systems containing pyridine moieties (**1ah** and **1aq**). For an overview of unsuccessful substrates, please see Table S10 in the supplemental methods.

METHODS

Further details regarding the experimental descriptions, general information, reagents, and information about all syntheses and characterizations are provided in the supplemental methods.

RESOURCE AVAILABILITY

Lead contact

Requests for further information and resources should be directed to and will be fulfilled by the lead contact, Xiaofeng Wei (xiaofeng.wei@xjtu.edu.cn).

Materials availability

Unless otherwise stated, reactions were carried out using dry solvents under a nitrogen atmosphere. Conversion was monitored by thin-layer chromatography (TLC) using Silicycle 200 mm silica gel GF-254 plates and visualized by UV light at 254 nm. Flash-column chromatography was performed over the silica gel (200–300 mesh). All NMR spectra were measured on JEOL JNM-ECZ400S/L1 and AVANCE III HD 600 spectrometers, NMR (400 MHz for ^{1}H-NMR and 101 MHz for ^{13}C-NMR). Chemical shifts are given in ppm, and the spectra are calibrated using the residual $CDCl_3$ or DMSO-d_6 signals. Multiplicities are abbreviated as follows: singlet (s), doublet (d), triplet (t), quartet (q), doublet of doublets (dd), doublet of triplets (dt), doublet of doublet of doublets (ddd), doublet of quartet (dq), triplet of doublets (td), multiplet (m), and broad (br). Chemical shifts of common trace ^{1}H-NMR impurities (ppm) are as follows: H_2O, 1.56; CH_2Cl_2, 5.31; and $CHCl_3$, 7.26. Infrared spectra were collected on a Bruker VERTEX70 as a thin attenuated total reflection, and the selected maximum absorbance was reported in wavenumbers. High-resolution mass spectra (HRMSs) were obtained on a Waters I-Class VION IMS QTof and are reported as *m*/*z* (relative intensity).

Data and code availability

- All experimental data supporting this article have been included as part of the supplemental methods.
- This paper does not report original code.
- Any additional information required to reanalyze the data reported in this paper is available from the lead contact upon request.

ACKNOWLEDGMENTS

We thank the High-Level Introduction Plan of Shaanxi Province, start-up funds from Xi'an Jiaotong University (XJTU), the National Natural Science Foundation of China (22571243 and 22101224), the National Natural Science Foundation of Shaanxi Province (2022JM-085), the Postdoctoral Fellowship Program (Grade C) of the China Postdoctoral Science Foundation (GZC20252344), the Shaanxi Provincial Postdoctoral Research Project, the Fundamental Research Funds for the Central Universities (xtr052025012 and xxj032025074), and the Zhejiang Provincial Natural Science Foundation of China (LMS25H160003). We also thank the Lawrencium computational cluster at Lawrence Berkeley National Laboratory (LBNL) for calculation support, Dr. C. Feng and Dr. G. Chang at the Instrument Analysis Center of XJTU for NMR analysis, and Mr. Li Guangping at the Shanghai Institute of Organic Chemistry for assistance with HRMS analysis.

AUTHOR CONTRIBUTIONS

C.F. and X.W. conceived the project; T.W., C.F., W.J., H.W., G.S., Y.G., J.S., and Y.Z. performed all experiments and analyzed all data; X.X., Y.S., M.K., K.A.P., and P.M. conducted the DFT calculations; and T.W., C.F., P.M., and X.W. wrote the manuscript with contributions from all authors.

DECLARATION OF INTERESTS

The authors declare no competing interests.

SUPPLEMENTAL INFORMATION

Supplemental information can be found online at https://doi.org/10.1016/j.xcrp.2025.103020.

Received: June 16, 2025
Revised: September 23, 2025
Accepted: November 18, 2025
Published: December 17, 2025

REFERENCES

1. Larock, R.C. (1999). Comprehensive Organic Transformations: A Guide to Functional Group Preparations, ed. 2 (VCH).
2. Larsen, C.R., and Grotjahn, D.B. (2017). The Value and Application of Transition Metal Catalyzed Alkene Isomerization in Industry. In Applied Homogeneous Catalysis with Organometallic Compounds: A Comprehensive Handbook in Four Volumes, B. Cornils, W.A. Herrman, M. Beller, and R. Paciello, eds. (Wiley), pp. 1365–1378.
3. Istvan, E.S., and Deisenhofer, J. (2001). Structural Mechanism for Statin Inhibition of HMG-CoA Reductase. Science *292*, 1160–1164. https://doi.org/10.1126/science.1059344.
4. Müller, M. (2005). Chemoenzymatic Synthesis of Building Blocks for Statin Side Chains. Angew. Chem. Int. Ed. *44*, 362–365.
5. Hung, D.T., Nerenberg, J.B., and Schreiber, S.L. (1996). Syntheses of Discodermolides Useful for Investigating Microtubule Binding and Stabilization. J. Am. Chem. Soc. *118*, 11054–11080. https://doi.org/10.1021/ja961374o.
6. Cornils, B. (2004). Modern Carbonyl Olefination. Methods and Applications. T. Takeda, ed. *43*, 3100–3101. https://doi.org/10.1002/anie.200385149.
7. Fürstner, A. (2019). trans-Hydrogenation, gem-Hydrogenation, and trans-Hydrometalation of Alkynes: An Interim Report on an Unorthodox Reactivity Paradigm. J. Am. Chem. Soc. *141*, 11–24. https://doi.org/10.1021/jacs.8b09782.
8. Nguyen, T.T., Koh, M.J., Shen, X., Romiti, F., Schrock, R.R., and Hoveyda, A.H. (2016). Kinetically Controlled *E*-Selective Catalytic Olefin Metathesis. Science *352*, 569–575. https://doi.org/10.1126/science.aaf4622.
9. Ahmed, T.S., and Grubbs, R.H. (2017). Fast-Initiating, Ruthenium-based Catalysts for Improved Activity in Highly *E*-Selective Cross Metathesis. J. Am. Chem. Soc. *139*, 1532–1537. https://doi.org/10.1021/jacs.6b11330.
10. Sai, M., and Matsubara, S. (2019). Copper-Catalyzed Direct and Stereoselective Synthesis of Conjugated Enynes from α-Allenols. Adv. Synth. Catal. *361*, 39–43. https://doi.org/10.1002/adsc.201801211.
11. Bodnar, A.K., and Newhouse, T.R. (2024). Accessing Z-Enynes via Cobalt-Catalyzed Propargylic Dehydrogenation. Angew. Chem. Int. Ed. *63*, e202402638. https://doi.org/10.1002/anie.202402638.
12. Pati, B.V., Ghosh, A., Yadav, K., Banjare, S.K., Pandey, S., Lourderaj, U., and Ravikumar, P.C. (2022). Palladium-Catalyzed Selective C–C Bond Cleavage and Stereoselective Alkenylation between Cyclopropanol and 1,3-Diyne: One-Step Synthesis of Diverse Conjugated Enynes. Chem. Sci. *13*, 2692–2700. https://doi.org/10.1039/D1SC04780A.
13. Chen, C., Dugan, T.R., Brennessel, W.W., Weix, D.J., and Holland, P.L. (2014). *Z*-Selective Alkene Isomerization by High-Spin Cobalt(II) Complexes. J. Am. Chem. Soc. *136*, 945–955. https://doi.org/10.1021/ja408238n.
14. Vasseur, A., Bruffaerts, J., and Marek, I. (2016). Remote functionalization through alkene isomerization. Nat. Chem. *8*, 209–219. https://doi.org/10.1038/nchem.2445.
15. Sommer, H., Juliá-Hernández, F., Martin, R., and Marek, I. (2018). Walking Metals for Remote Functionalization. ACS Cent. Sci. *4*, 153–165. https://doi.org/10.1021/acscentsci.8b00005.
16. Chang, A.S.-m., Kascoutas, M.A., Valentine, Q.P., How, K.I., Thomas, R.M., and Cook, A.K. (2024). Alkene Isomerization Using a Heterogeneous Nickel-Hydride Catalyst. J. Am. Chem. Soc. *146*, 15596–15608. https://doi.org/10.1021/jacs.4c04719.
17. Garhwal, S., Kaushansky, A., Fridman, N., and de Ruiter, G. (2021). Part per million levels of an anionic iron hydride complex catalyzes selective alkene isomerization via two-state reactivity. Chem Catal. *1*, 631–647. https://doi.org/10.1016/j.checat.2021.05.002.
18. Molloy, J.J., Morack, T., and Gilmour, R. (2019). Positional and Geometrical Isomerisation of Alkenes: The Pinnacle of Atom Economy. Angew. Chem. Int. Ed. *58*, 13654–13664. https://doi.org/10.1002/anie.201906124.
19. Segura, L., Massad, I., Ogasawara, M., and Marek, I. (2021). Stereodivergent Access to Trisubstituted Alkenylboronate Esters through Alkene Isomerization. Org. Lett. *23*, 9194–9198. https://doi.org/10.1021/acs.orglett.1c03513.
20. Biswas, S. (2015). Mechanistic Understanding of Transition-Metal-Catalyzed Olefin Isomerization: Metal-Hydride Insertion-Elimination vs. π--Allyl Pathways. Comments Inorg. Chem. *35*, 300–330. https://doi.org/10.1080/02603594.2015.1059325.
21. Massad, I., and Marek, I. (2020). Alkene Isomerization through Allylmetals as a Strategic Tool in Stereoselective Synthesis. ACS Catal. *10*, 5793–5804. https://doi.org/10.1021/acscatal.0c01174.
22. Kim, D., Pillon, G., DiPrimio, D.J., and Holland, P.L. (2021). Highly Z-Selective Double Bond Transposition in Simple Alkenes and Allylarenes through a Spin-Accelerated Allyl Mechanism. J. Am. Chem. Soc. *143*, 3070–3074. https://doi.org/10.1021/jacs.1c00856.
23. Kapat, A., Sperger, T., Guven, S., and Schoenebeck, F. (2019). *E*-Olefins through Intramolecular Radical Relocation. Science *363*, 391–396. https://doi.org/10.1126/science.aav1610.
24. Crossley, S.W.M., Barabé, F., and Shenvi, R.A. (2014). Simple, Chemoselective, Catalytic Olefin Isomerization. J. Am. Chem. Soc. *136*, 16788–16791. https://doi.org/10.1021/ja5105602.
25. Crossley, S.W.M., Obradors, C., Martinez, R.M., and Shenvi, R.A. (2016). Mn-Fe-and Co-Catalyzed Radical Hydrofunctionalizations of Olefins. Chem. Rev. *116*, 8912–9000. https://doi.org/10.1021/acs.chemrev.6b00334.
26. Li, G., Kuo, J.L., Han, A., Abuyuan, J.M., Young, L.C., Norton, J.R., and Palmer, J.H. (2016). Radical Isomerization and Cycloisomerization Initiated by H· Transfer. J. Am. Chem. Soc. *138*, 7698–7704. https://doi.org/10.1021/jacs.6b03509.
27. Green, S.A., Crossley, S.W.M., Matos, J.L.M., Vásquez-Céspedes, S., Shevick, S.L., and Shenvi, R.A. (2018). The High Chemofidelity of Metal-Catalyzed Hydrogen Atom Transfer. Acc. Chem. Res. *51*, 2628–2640. https://doi.org/10.1021/acs.accounts.8b00337.
28. Gnaim, S., Bauer, A., Zhang, H.-J., Chen, L., Gannett, C., Malapit, C.A., Hill, D.E., Vogt, D., Tang, T., Daley, R.A., et al. (2022). Cobalt-Electrocatalytic HAT for Functionalization of Unsaturated C–C Bonds. Nature *605*, 687–695. https://doi.org/10.1038/s41586-022-04595-3.
29. Rubel, C.Z., Ravn, A.K., Ho, H.C., Yang, S., Li, Z.-Q., Engle, K.M., and Vantourout, J.C. (2024). Stereodivergent, Kinetically Controlled Isomerization of Terminal Alkenes via Nickel Catalysis. Angew. Chem. Int. Ed. *63*, e202320081. https://doi.org/10.1002/anie.202320081.
30. Ohmura, T., Oshima, K., and Suginome, M. (2011). , (E)- and (Z)-β-Borylallylsilanes by Alkyne Silaboration Followed by Regio- and Stereoselective Double-Bond Migration. Angew. Chem. Int. Ed. *50*, 12501–12504. https://doi.org/10.1002/anie.201106077.

31. Jankins, T.C., Rubel, C.Z., Ho, H.C., Martin-Montero, R., and Engle, K.M. (2025). Tungsten-catalyzed stereodivergent isomerization of terminal olefins. Chem. Sci. *16*, 2307–2315. https://doi.org/10.1039/D4SC07093C.

32. Carvalho-Junior, E.J., and Oliveira, C. (2022). Nickel-Catalyzed Double Bond Transposition under Kinetic Control. Preprint at ChemRxiv. https://doi.org/10.26434/chemrxiv-2022-w9n02.

33. Iverson, S.L., and Uetrecht, J.P. (2001). Identification of a Reactive Metabolite of Terbinafine: Insights into Terbinafine-Induced Hepatotoxicity. Chem. Res. Toxicol. *14*, 175–181. https://doi.org/10.1021/tx0002029.

34. Zhou, Y., Zhang, Y., and Wang, J. (2016). Recent advances in transition-metal-catalyzed synthesis of conjugated enynes. Org. Biomol. Chem. *14*, 6638–6650. https://doi.org/10.1039/C6OB00944A.

35. Dwiecki, P.M., Michalak, T.K., and Muszalska-Kolos, I. (2022). Assessment of the Properties of Terbinafine Hydrochloride and the Search Route for Antifungal Agents. J. Mol. Struct. *1252*, 132225. https://doi.org/10.1016/j.molstruc.2021.132225.

36. Zhang, H.J., Sydara, K., Tan, G.T., Ma, C., Southavong, B., Soejarto, D.D., Pezzuto, J.M., and Fong, H.H.S. (2004). Bioactive Constituents from Asparagus cochinchinensis. J. Nat. Prod. *67*, 194–200. https://doi.org/10.1021/np030370b.

37. Yi, C.S., and Liu, N. (1996). Homogeneous Catalytic Dimerization of Terminal Alkynes by $C_5Me_5Ru(L)H_3$ (L = PPh_3, PCy_3, PMe_3). Organometallics *15*, 3968–3971. https://doi.org/10.1021/om9601110.

38. N., Y. C. a. L. (1999). Synlett, 281–287.

39. Xue, F., Song, X., Lin, T.T., Munkerup, K., Albawardi, S.F., Huang, K.W., Hor, T.S.A., and Zhao, J. (2018). Dimerization of Terminal Aryl Alkynes Catalyzed by Iron(II) Amine-Pyrazolyl Tripodal Complexes with E/Z Selectivity Controlled by tert-Butoxide. ACS Omega *3*, 5071–5077. https://doi.org/10.1021/acsomega.8b00539.

40. Shibasaki, M., and Kanai, M. (2008). Asymmetric Synthesis of Tertiary Alcohols and α-Tertiary Amines via Cu-Catalyzed C−C Bond Formation to Ketones and Ketimines. Chem. Rev. *108*, 2853–2873. https://doi.org/10.1021/cr078340r.

41. Li, H., and Yin, L. (2022). Research Progress of Copper-Catalyzed Direct Vinylogous Reactions. Chinese J. Org. Chem. *42*, 1573–1585. https://doi.org/10.6023/cjoc202201033.

42. Yazaki, R., Kumagai, N., and Shibasaki, M. (2009). Direct Catalytic Asymmetric Addition of Allyl Cyanide to Ketones. J. Am. Chem. Soc. *131*, 3195–3197. https://doi.org/10.1021/ja900001u.

43. Wei, X.F., Xie, X.W., Shimizu, Y., and Kanai, M. (2017). Copper(I)-Catalyzed Enantioselective Addition of Enynes to Ketones. J. Am. Chem. Soc. *139*, 4647–4650. https://doi.org/10.1021/jacs.7b01254.

44. Zhang, H.J., and Yin, L. (2018). Asymmetric Synthesis of α,β-Unsaturated δ-Lactones through Copper(I)-Catalyzed Direct Vinylogous Aldol Reaction. J. Am. Chem. Soc. *140*, 12270–12279. https://doi.org/10.1021/jacs.8b07929.

45. Zhong, F., Pan, Z.Z., Zhou, S.W., Zhang, H.J., and Yin, L. (2021). Copper(I)-Catalyzed Regioselective Asymmetric Addition of 1,4-Pentadiene to Ketones. J. Am. Chem. Soc. *143*, 4556–4562. https://doi.org/10.1021/jacs.1c02084.

46. Wei, X.F., Wakaki, T., Itoh, T., Li, H.L., Yoshimura, T., Miyazaki, A., Oisaki, K., Hatanaka, M., Shimizu, Y., and Kanai, M. (2019). Catalytic Regio- and Enantioselective Proton Migration from Skipped Enynes to Allenes. Chem *5*, 585–599. https://doi.org/10.1016/j.chempr.2018.11.022.

47. Bieber, L.W., and da Silva, M.F. (2007). Copper Catalyzed Regioselective Coupling of Allylic Halides and Alkynes Promoted by Weak Inorganic Bases. Tetrahedron Lett. *48*, 7088–7090. https://doi.org/10.1016/j.tetlet.2007.08.010.

48. Zhou, H., and Moberg, C. (2013). Regio- and Stereoselective Hydrosilylation of 1,3-Enynes Catalyzed by Palladium. Org. Lett. *15*, 1444–1447. https://doi.org/10.1021/ol4001334.

49. Jia, Y., Yang, L., Wang, X., Yang, W., and Zhao, W. (2024). Cobalt-Catalyzed Selective Hydroboration of 1,3-Enynes with HBpin toward 1,3-Dienylboronate Esters. Org. Lett. *26*, 3258–3262. https://doi.org/10.1021/acs.orglett.4c00899.

50. Liao, S., and List, B. (2010). Asymmetric Counteranion-Directed Transition-Metal Catalysis: Enantioselective Epoxidation of Alkenes with Manganese(III) Salen Phosphate Complexes. Angew. Chem. Int. Ed. *49*, 628–631. https://doi.org/10.1002/anie.200905332.

51. González, M.J., González, J., and Vicente, R. (2012). An Alternative Reaction Outcome in the Gold-Catalyzed Rearrangement of 1-Alkynyloxiranes. Eur. J. Org. Chem. *2012*, 6140–6143. https://doi.org/10.1002/ejoc.201201191.

52. Odedra, A., Wu, C.-J., Madhushaw, R.J., Wang, S.-L., and Liu, R.-S. (2003). A New Co2(CO)8-Mediated Tandem [5 + 1]/[2 + 2 + 1]-Cycloaddition Reaction: A One-Pot Synthesis of Tricyclic δ-Lactones from cis-Epoxy Ene-ynes. J. Am. Chem. Soc. *125*, 9610–9611. https://doi.org/10.1021/ja0346633.

53. Rudisill, D.E., Castonguay, L.A., and Stille, J.K. (1988). Synthesis of Terbinafine. A Palladium Catalyzed Vinyl Iodide-Ethynylstannane Coupling. Tetrahedron Lett. *29*, 1509–1512. https://doi.org/10.1016/S0040-4039(00)80338-X.

54. Alami, M., Ferri, F., and Gaslain, Y. (1996). A Two-Step Synthesis of Terbinafine. Tetrahedron Lett. *37*, 57–58. https://doi.org/10.1016/0040-4039(95)02095-0.

55. Sauerberg, P., Bury, P.S., Mogensen, J.P., Deussen, H.-J., Pettersson, I., Fleckner, J., Nehlin, J., Frederiksen, K.S., Albrektsen, T., Din, N., et al. (2003). Large Dimeric Ligands with Favorable Pharmacokinetic Properties and Peroxisome Proliferator-Activated Receptor Agonist Activity in Vitro and in Vivo. J. Med. Chem. *46*, 4883–4894. https://doi.org/10.1021/jm0309046.

56. Deussen, H.-J., Jeppesen, L., Schärer, N., Junager, F., Bentzen, B., Weber, B., Weil, V., Mozer, S.J., and Sauerberg, P. (2004). Process Development and Scale-Up of the PPAR Agonist NNC 61-4655. Org. Process. Res. Dev. *8*, 363–371. https://doi.org/10.1021/op034048j.

57. Campbell, K., Kuehl, C.J., Ferguson, M.J., Stang, P.J., and Tykwinski, R.R. (2002). Coordination-Driven Self-Assembly: Solids with Bidirectional Porosity. J. Am. Chem. Soc. *124*, 7266–7267. https://doi.org/10.1021/ja025773x.

58. El-Jaber, N., Estévez-Braun, A., Ravelo, A.G., Muñoz-Muñoz, O., Rodríguez-Afonso, A., and Murguia, J.R. (2003). Acetylenic Acids from the Aerial Parts of Nanodea muscosa. J. Nat. Prod. *66*, 722–724. https://doi.org/10.1021/np020513e.

59. Fontana, A., d'Ippolito, G., D'Souza, L., Mollo, E., Parameswaram, P.S., and Cimino, G. (2001). New Acetogenin Peroxides from the Indian Sponge Acarnus bicladotylota. J. Nat. Prod. *64*, 131–133. https://doi.org/10.1021/np0002435.

60. Xiao, N., Zhan, Y.-Z., Meng, H., and Shu, W. (2021). Access to Z-Selective 1,3-Enynes via Ni-Catalyzed Intermolecular Cross-Alkylalkynylation of Terminal Alkynes. Org. Lett. *23*, 5186–5191. https://doi.org/10.1021/acs.orglett.1c01728.

61. Trost, B.M., and Masters, J.T. (2016). Transition metal-catalyzed couplings of alkynes to 1,3-enynes: modern methods and synthetic applications. Chem. Soc. Rev. *45*, 2212–2238. https://doi.org/10.1039/C5CS00892A.

62. Huang, F., Huang, Z., Liu, G., and Huang, Z. (2022). Iridium-Catalyzed Selective trans-Semihydrogenation of 1,3-Enynes with Ethanol: Access to (E,E)-1,4-Diarylbutadienes. Org. Lett. *24*, 5486–5490. https://doi.org/10.1021/acs.orglett.2c02327.

63. Manna, S., Dherbassy, Q., Perry, G.J.P., and Procter, D.J. (2020). Enantio- and Diastereoselective Synthesis of Homopropargyl Amines by Copper-Catalyzed Coupling of Imines, 1,3-Enynes, and Diborons. Angew. Chem. Int. Ed. *59*, 4879–4882. https://doi.org/10.1002/anie.201915191.

64. Lu, W., Zhao, Y., and Meng, F. (2022). Cobalt-Catalyzed Sequential Site- and Stereoselective Hydrosilylation of 1,3- and 1,4-Enynes. J. Am. Chem. Soc. *144*, 5233–5240. https://doi.org/10.1021/jacs.2c00288.

65. Yue, X., Hu, M., He, X., Wu, S., and Li, J.H. (2020). A Radical-Mediated 1,3,4-Trifunctionalization Cascade of 1,3-Enynes with Sulfinates and Tert-Butyl Nitrite: Facile Access to Sulfonyl Isoxazoles. Chem. Commun. *56*, 6253–6256. https://doi.org/10.1039/D0CC01659D.

66. Zhou, Y., Zhou, L., Jesikiewicz, L.T., Liu, P., and Buchwald, S.L. (2020). Synthesis of Pyrroles through the CuH-Catalyzed Coupling of Enynes and Nitriles. J. Am. Chem. Soc. *142*, 9908–9914. https://doi.org/10.1021/jacs.0c03859.

67. Peng, C., Wu, T., Yang, X., Pei, M., Wang, S., Kanai, M., Shimizu, Y., and Wei, X. (2024). Copper(I)-Catalyzed Asymmetric Nucleophilic Addition to Aldehydes with Skipped Enynes. Org. Lett. *26*, 10072–10077. https://doi.org/10.1021/acs.orglett.4c03449.

68. Zhong, F., Xue, Q.Y., and Yin, L. (2020). Construction of Chiral 2,3-Allenols through a Copper(I)-Catalyzed Asymmetric Direct Alkynylogous Aldol Reaction. Angew. Chem. Int. Ed. *59*, 1562–1566. https://doi.org/10.1002/anie.201912140.

69. Wang, H., Luo, H., Zhang, Z.M., Zheng, W.F., Yin, Y., Qian, H., Zhang, J., and Ma, S. (2020). Pd-Catalyzed Enantioselective Syntheses of Trisubstituted Allenes via Coupling of Propargylic Benzoates with Organoboronic Acids. J. Am. Chem. Soc. *142*, 9763–9771. https://doi.org/10.1021/jacs.0c02876.

70. Sang, H.L., Yu, S., and Ge, S. (2018). Copper-catalyzed asymmetric hydroboration of 1,3-enynes with pinacolborane to access chiral allenylboronates. Org. Chem. Front. *5*, 1284–1287. https://doi.org/10.1039/C8QO00167G.